Development and Research of GOES-R ABI all sky radiance data assimilation for rapidly evolving convective scale weather prediction

Aaron Johnson, Xuguang Wang, Krishna Chandramouli
Multiscale data Assimilation and Predictability (MAP) Lab
University of Oklahoma, Norman, OK

In collaboration with
Thomes Jones (CIWRO) and Jason Otkins (CIMSS)

6 December 2021
CIWRO Mesoscale and Stormscale Modeling R&D Workshop

Background and Motivation

- High time and space resolution of ABI is well suited for DA of rapidly evolving, small scale convective systems.

- ABI and radar observations can provide complementary information about storm structure.

- While previous studies have demonstrated advantages of assimilating all sky (clear and cloudy) radiances for convective scales (e.g., Minamide and Zhang 2019; Zhang et al. 2019), large room still exists to optimize the assimilation, which requires new methodological development and evaluation: e.g.,
  - Past studies only limit to assimilating one ABI channel
  - Further exploration of methods to treat system errors of the ensemble based DA approach for ABI radiance assimilation is still needed
  - Further exploration of methods to estimate ABI radiance observation errors is still needed
  - Past studies have shown the superiority of online bias correction with anchoring observation in the context of clear-sky radiance assimilation for global NWP. (e.g., Auligne et al. 2007). However, so far only the offline method is implemented to remove complex bias present in all-sky radiance observations for convective scale data assimilation. (Otkin et al. 2018, Johnson et al. 2021)

- Herein, OU MAP lab proposed, developed and evaluated the following techniques for the assimilation of ABI all sky radiance for a case study of rapidly developing supercells:
  - Additive inflation based on observed cloud where none is forecast
  - Adaptive observation error estimation for all-sky ABI radiance
  - Inclusion of different ABI water vapor channels individually and simultaneously
  - Online nonlinear bias correction using radar reflectivity as anchoring observation

Outline

- Case study overview
- Part 1: Additive inflation, adaptive observation error, and different ABI channels (Johnson et al 2021)
- Part 2: offline vs. online nonlinear bias correction (Chandramouli et al. 2021)
- Summary and plans

Case study overview

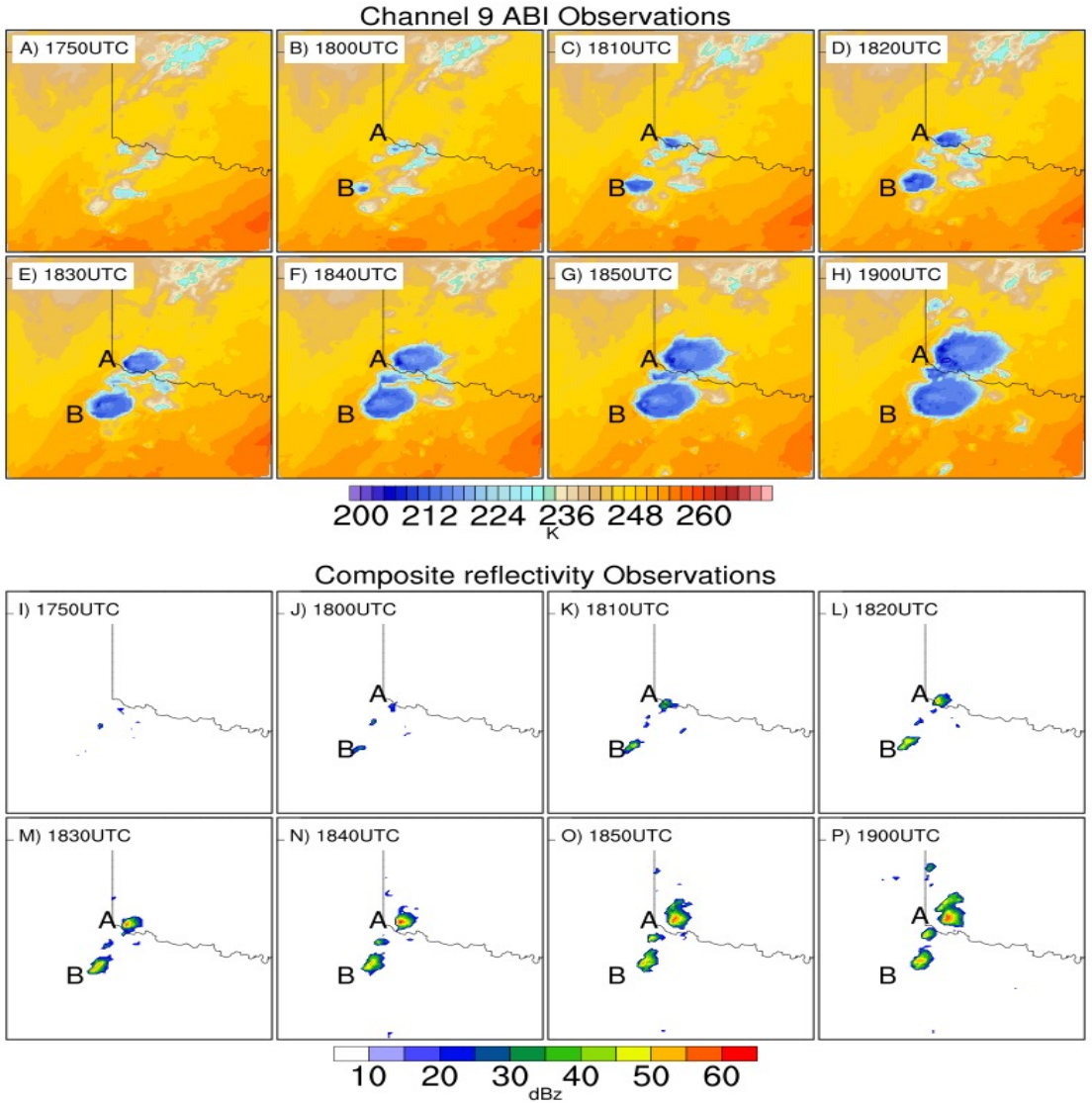

- A rapidly developing supercell event of May 18, 2017, was selected.
- Conducive dry line along with the upper-level trough led to the formation of multiple supercells
- ABI channel 9 observations sense the formation of towering cumulus clouds before the strong reflectivity signatures (≧35 dBz) are seen in RADAR observations
- The two storms that initiated around 1800 UTC (labelled as A and B in Figure) developed into long-lived supercells.

Outline

- Case study overview
- Part 1: Additive inflation, adaptive observation error, and different ABI channels (Johnson et al. 2021)
- Part 2: offline vs. online nonlinear bias correction (Chandramouli et al. 2021)
- Summary and plans

Method: adaptive observation error

- Default observation error is 1 K for ABI and 5 dBZ for reflectivity
- Adaptive observation error for ABI is implemented using first guess statistics, binned by symmetric cloud affect.
- First, a brightness temperature (BT) threshold is determined to approximately separate cloud-affected from cloud-free pixels (Harnisch et al. 2016).
- Then, cloud affect on forecast (C_f) and observed (C_o) radiances is calculated as:

  $C_f=\max[0,BT_{lim}-BT_f]$ and $C_o=\max[0,BT_{lim}-(BT_o-\beta)$, where beta is overall bias of BT_o relative to BT_f
- The symmetric cloud affect, $C=(C_f+C_o)/2$ is used to bin innovation statistics.
- Within each bin, the bias-corrected RMSI ($RMSI_{bc}$) is known and the forecast error variance (σ_f^2) is approximated using the ensemble variance (σ_e^2), so the observation error variance (σ_o^2) is estimated using:

$$RMSI_{bc} \approx \sqrt{\sigma_o^2 + \sigma_e^2}$$

- While this is not a perfect approximation given the under-dispersive ensemble, the effectiveness of the approximation for data assimilation can be evaluated indirectly through impact on skill of forecast initialized from ensemble mean analysis.

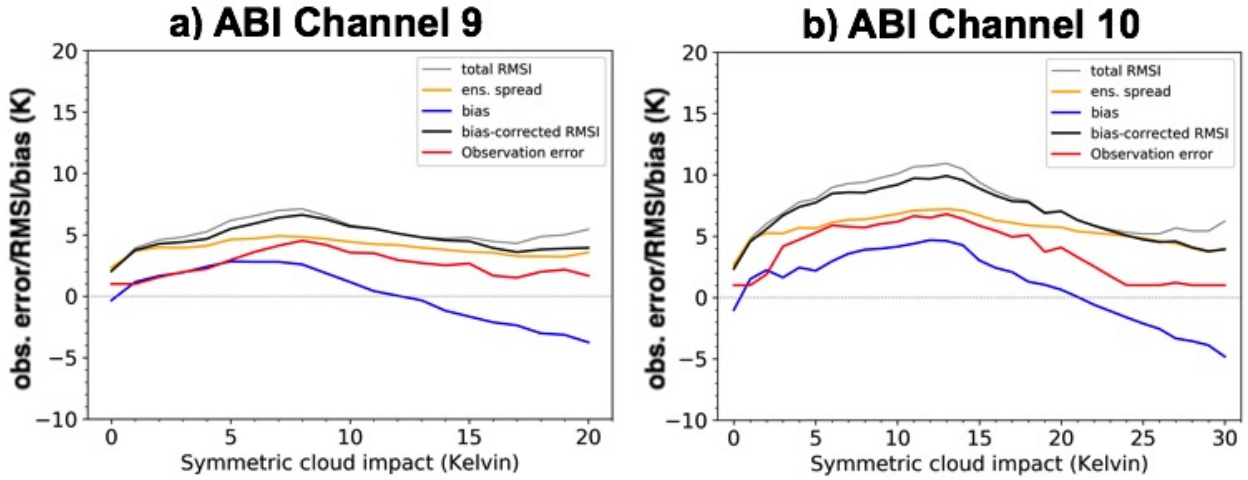

Method: additive inflation

- Inspired by radar reflectivity assimilation (e.g., Dowell and Wicker 2009; Wang and Wang 2017, 2020a), an additive inflation approach is developed for the ABI radiance assimilation to treat the system errors in ensemble DA.
- Applied for cloudy observed pixels (C_o>2K) which are cloud-free in background forecast (C_f<2K).
- Random perturbations are applied to each ensemble member at nearest grid point (below 500 hPa) with standard deviation of 0.25 K, 0.25 K and 0.25 ms^{-1} for temperature, dewpoint, and wind, respectively.
- The practical effect of perturbations is to help trigger storm initiation in the next background forecast after deep clouds start to appear in ABI radiance observations.

Experiment design

- GSI based EnKF extended for convective scale data assimilation system by OU MAP (Johnson et al. 2015, Wang and Wang 2017).

- Conventional observations assimilated hourly from 0000-1600 UTC.
- Radar reflectivity only assimilated every 10 min from 1610-1700 (suppression of spurious convection).
- Experiments with different techniques of assimilating ABI radiance start 1710 UTC.
- Two ABI channels, 9 and 10 are assimilated

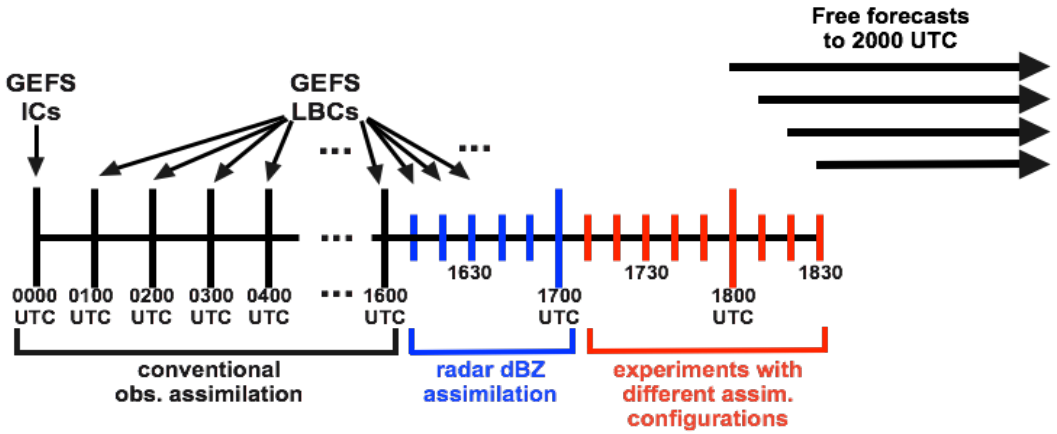

Experiment	Add. Infl.	dBZ	Ch. 9	Ch. 10	Obs. error	BG ensemble
radaronly	N	Y	N	N		
Ch10	N	Y	N	Y	1 K	
Ch10_addn	Y	Y	N	Y	1 K	
Ch10_addn_obserr	Y	Y	N	Y	Adaptive	
Ch9_addn_obserr	Y	Y	Y	N	Adaptive	
Ch9ch10_addn_obserr	Y	Y	Y	Y	Adaptive	
Ch9_addn_obserr_1750bg	Y	Y	Y	N	Adaptive	Ch10_addn_obserr
Ch10_addn_obserr_1750bg	Y	Y	N	Y	Adaptive	Ch9_addn_obserr

Johnson et al. (2021; JGR-atmos.)

Impact of adaptive observation error and additive inflation

- Additive inflation adds about 20 minutes of forecast lead time to southern storm.
- Adaptive observation error is most beneficial for early (1810 UTC) forecasts of northern storm and maintaining intensity of both storms at 1830 UTC.
- Qualitative inspection of background error covariance structure at different parts of storm (not shown) was used to interpret impact of adaptive observation error.
- As storm matures and anvil spreads, covariances for reflectivity are more consistent with expected storm structure than ABI covariances which don't distinguish updraft from non-updraft beneath the anvil.
- As ABI observation error is increased during this period of spreading anvil, the reflectivity observations have greater contribution to DA increment.

Johnson et al. (2021; JGR-atmos.)

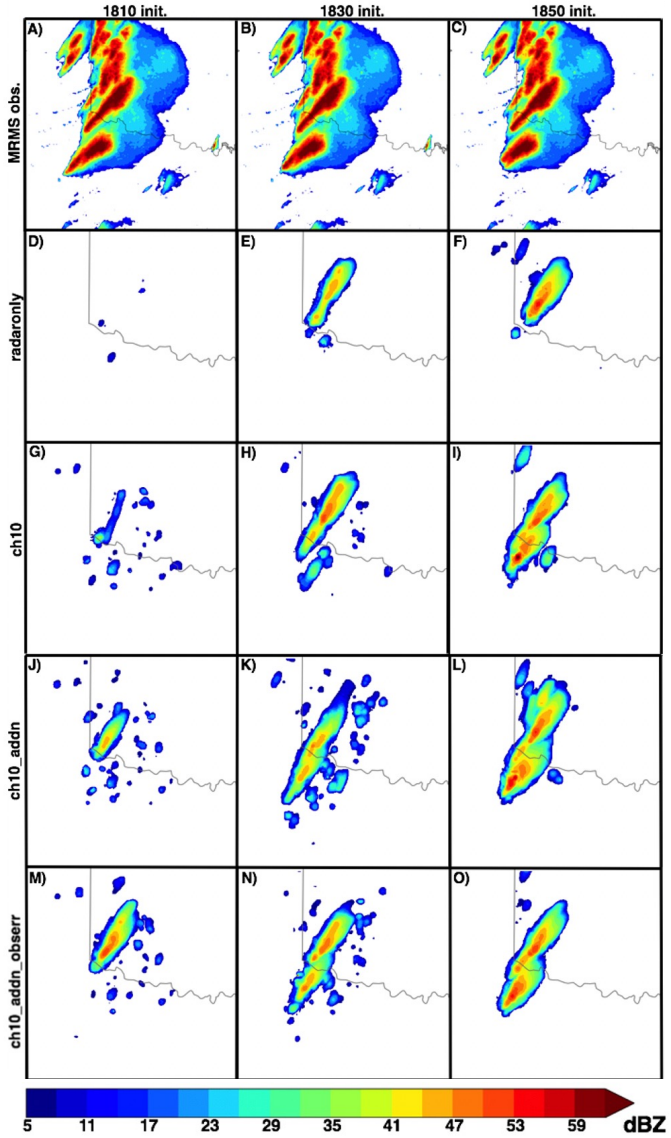

Time-maximum composite reflectivity during the period from the forecast initialization time through 2000 UTC

Impact of different ABI channels

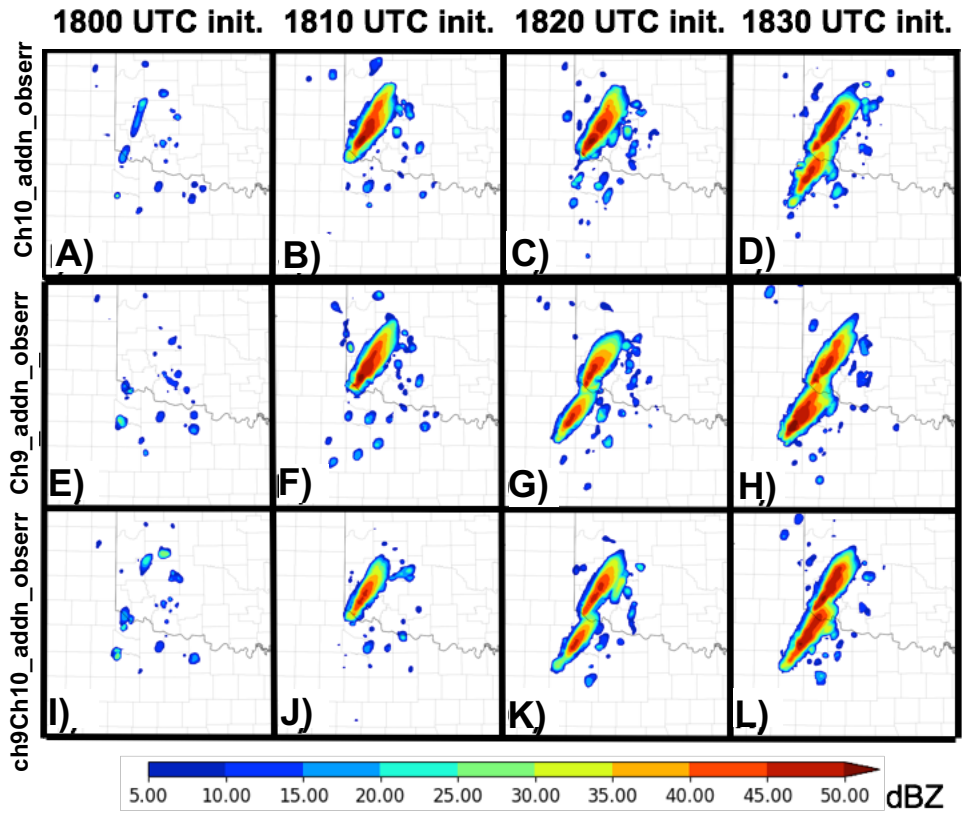

- Experiments including Channel 9 pick up on southern storm one cycle earlier than experiment with Ch. 10 only.
- Swapping ensembles at 1750, results in Channel 10 experiment picking up on southern storm earlier.
  - This shows that the difference comes from the earlier cycles before convection initiates.
- While 10 minutes is a small difference, it is physically consistent with a stronger upper-level shortwave in experiments assimilating ch9 than ch10.
  - Correlation between upper level water vapor and vorticity in shortwave

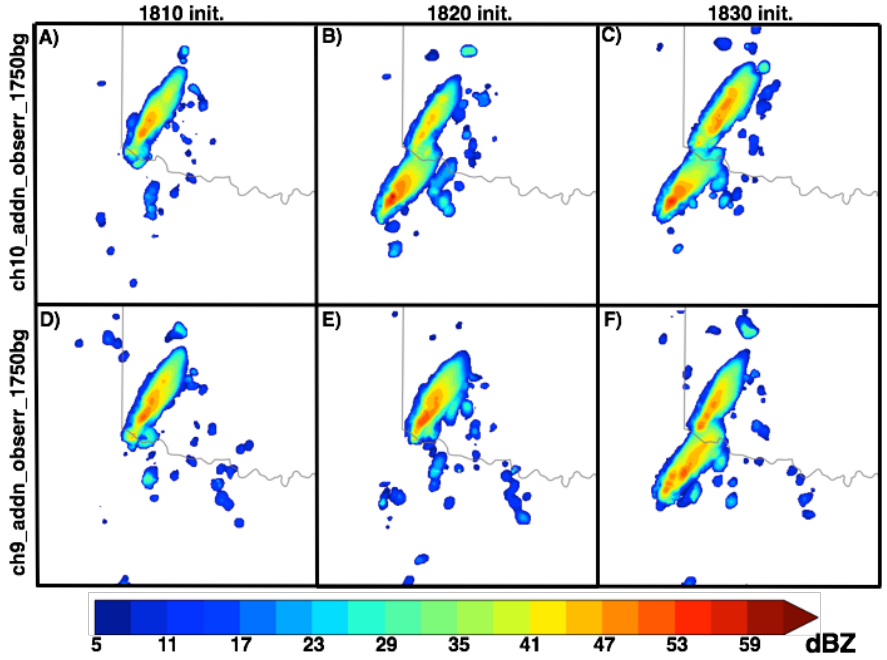

Outline

- Case study overview
- Part 1: Additive inflation, adaptive observation error, and different ABI channels (Johnson et al. 2021)
- Part 2: offline vs. online nonlinear bias correction (Chandramouli et al. 2021)
- Summary and plans

Bias correction approaches

- **Non-linear offline bias correction:**

  - Statistics of first-guess departures (O-B) are used to estimate the bias.
  - Can not distinguish bias in the obs and bias in the model
  - The non-linear offline approach by Otkin et al. (2018) represents fitting a polynomial function of bias predictors to the model first-guess departure

- **Non-linear online bias correction:**

  - The bias is estimated at each analysis step along with the estimated state, i.e. update of bias and state are coupled (Fertig et al. 2009).
  - Past studies have revealed the co-existence of an unbiased anchor observation along with bias corrected observation can help distinguish the model and observation component of the biases, which in turn gives better analysis and forecast (Eyre 2016).
  - We further implemented the non-linear cubic polynomial function for ABI radiances similar to the offline approach in the EnKF online bias correction framework

Bias correction approaches
Practical consideration

- For the rapidly cycled ABI radiance DA experiments, RADAR reflectivity is served as anchor observation.

- RADAR reflectivity and ABI radiances are sensitive to different variables and contribute to the analysis increment in different regions of the cloud. However, RADAR reflectivity and ABI cloud sensitive radiances are physically connected.

- <u>RADAR can act as anchor:</u>
  - ✓ The increments created by RADAR on precipitating hydrometeors and updrafts at low- and mid-levels are physically linked to the formation of high-level clouds which are seen by ABI radiances .
  - ✓ Similarly, the increments created by RADAR on spurious precipitation also affects the suppression of high-level spurious clouds which are seen by ABI radiances.

- <u>RADAR cannot act as anchor :</u>
  - ✓ In the regions where both the model and observations have non-precipitating clouds, RADAR reflectivity can not serve as an anchor because the innovation for RADAR reflectivity observation is zero. Over such regions, no bias correction is currently applied.
  - ✓ In the cloud free regions, the humidity increments created by ABI radiances are not constrained by the RADAR reflectivity observations as RADAR is sensitive only to precipitating hydrometeors.

- The bias coefficients for both non-linear offline and online bias correction are calculated and applied over ABI radiances in the vicinity of RADAR anchored region.

Offline vs Online bias correction

Analysis

Channel 9 BT analysis

offline

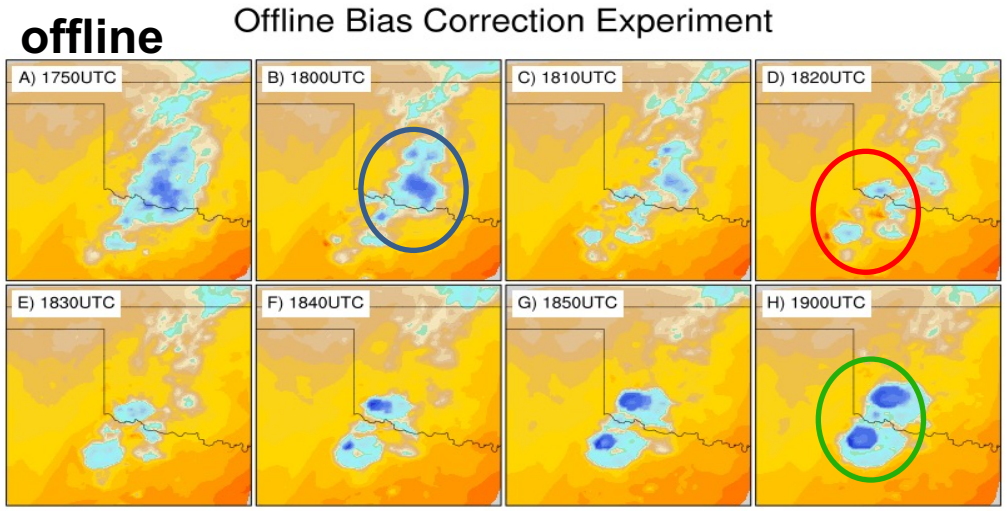

online

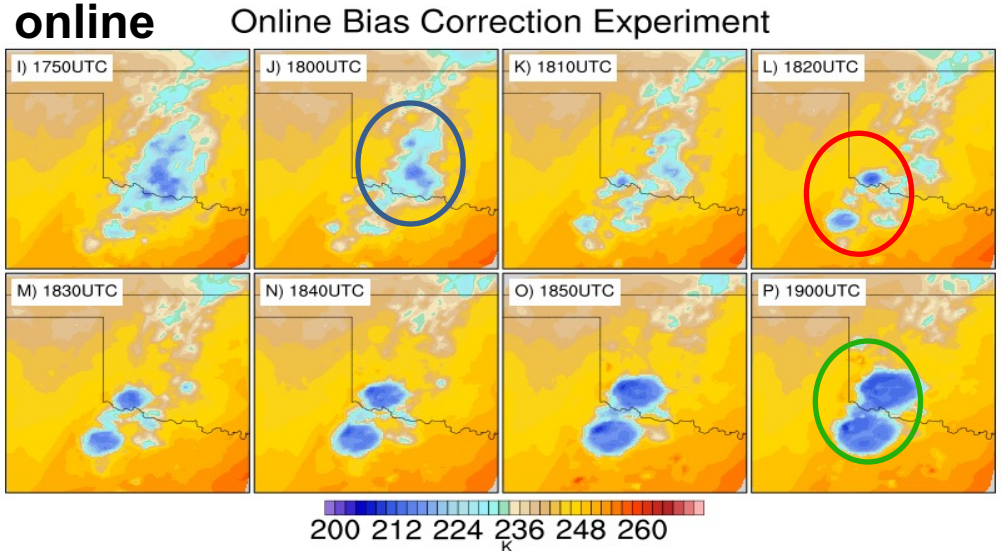

obs

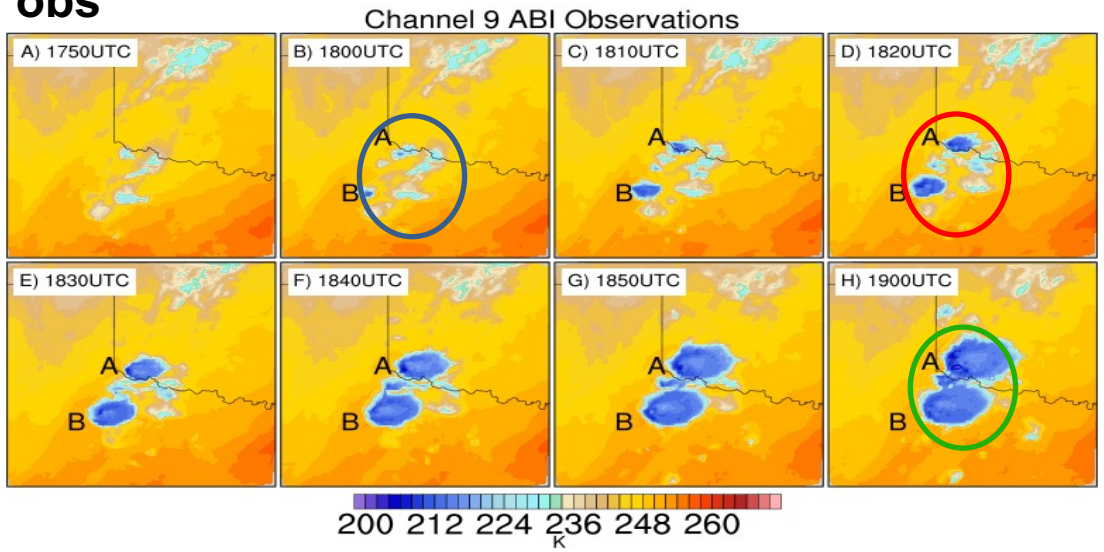

- In comparison to offline approach, the spurious clouds are suppressed relatively more effectively in an online bias correction.
- The analysis of the online bias correction approach more closely matches the observed rapid development of the supercell storms.

Chandramouli et al. (2021; JAMES)

Offline vs Online bias correction

Analysis & first guess fit to obs

ABI over observed cloud region

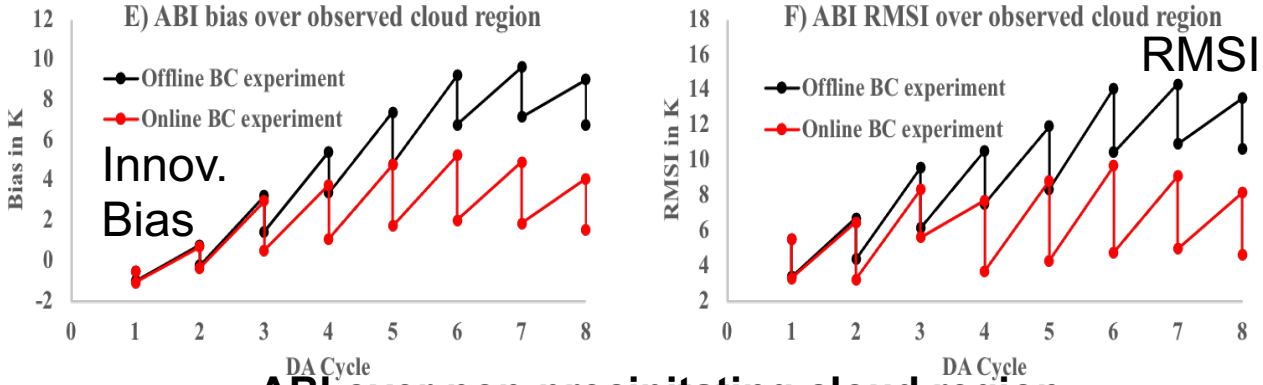

ABI over non-precipitating cloud region

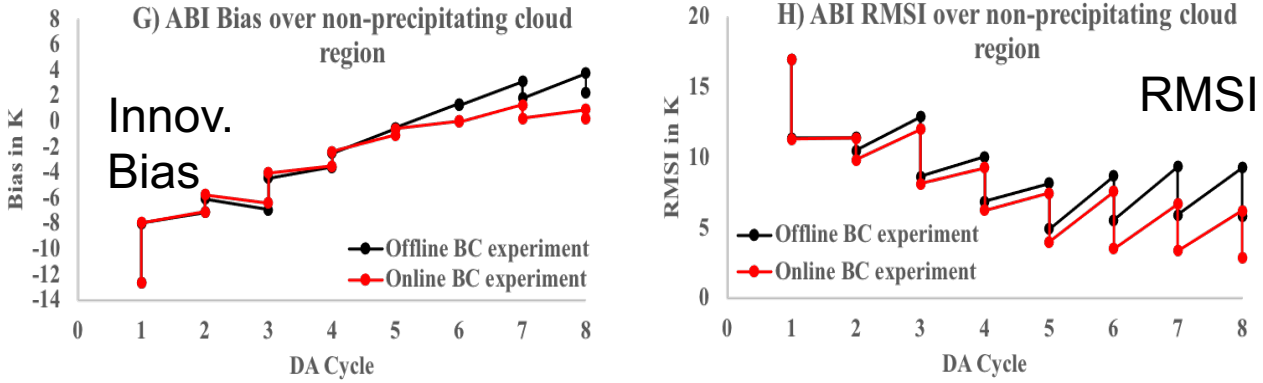

Suppression of spurious cloud

Establishment of storms

Suppression of spurious cloud

Establishment of storms

- ❑ As the storm intensifies, the first guess of the online approach fits the observed cloud more closely than offline approach.
- ❑ Although radar anchors precip. region, the first guess of the online bias correction fits the non-precipitating cloud more closely than the offline approach:
- ✓ Improvements in bias/RMSI are seen in suppression of spurious non-precipitation clouds.
- ✓ Online approach is able to spin up new non-precipitating clouds faster in the analysis from 1840UTC, which is reflected in both bias and RMSI.

Chandramouli et al. (2021; JAMES)

Offline vs Online bias correction

Forecast

Comparison of RADAR reflectivity swath forecasts

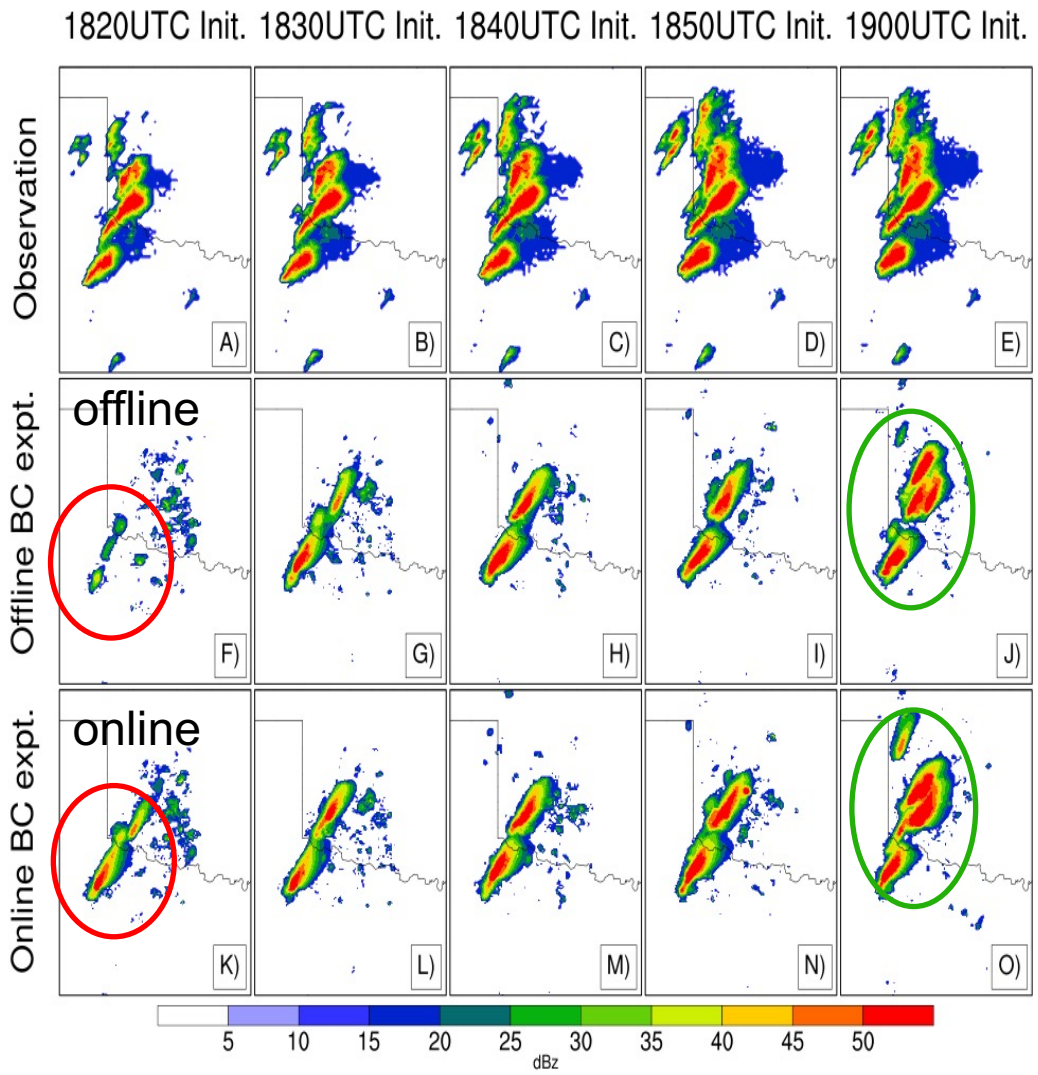

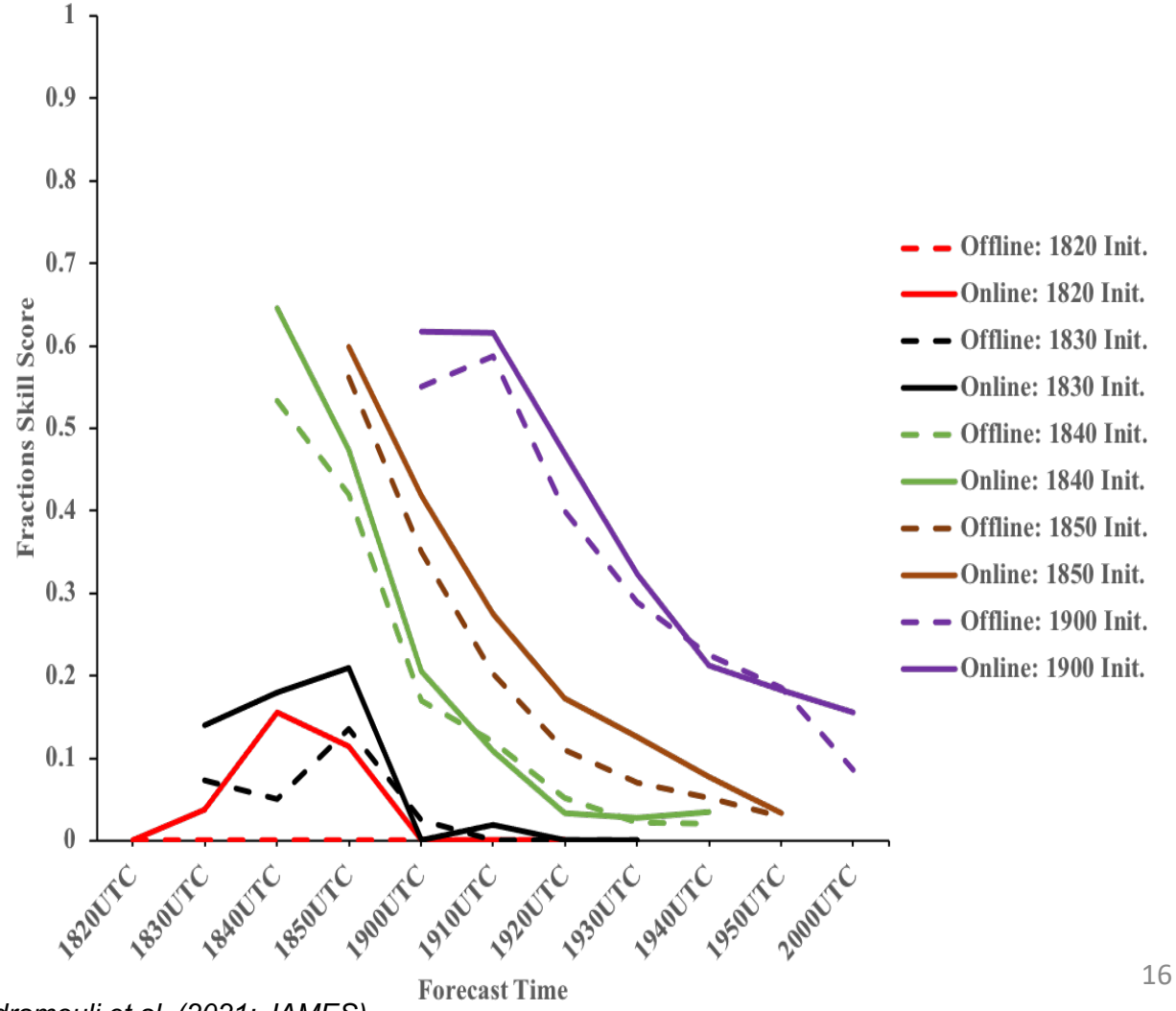

Chandramouli et al. (2021; JAMES)

Physical diagnostics

Bias corrected Channel 9 radiance innovation

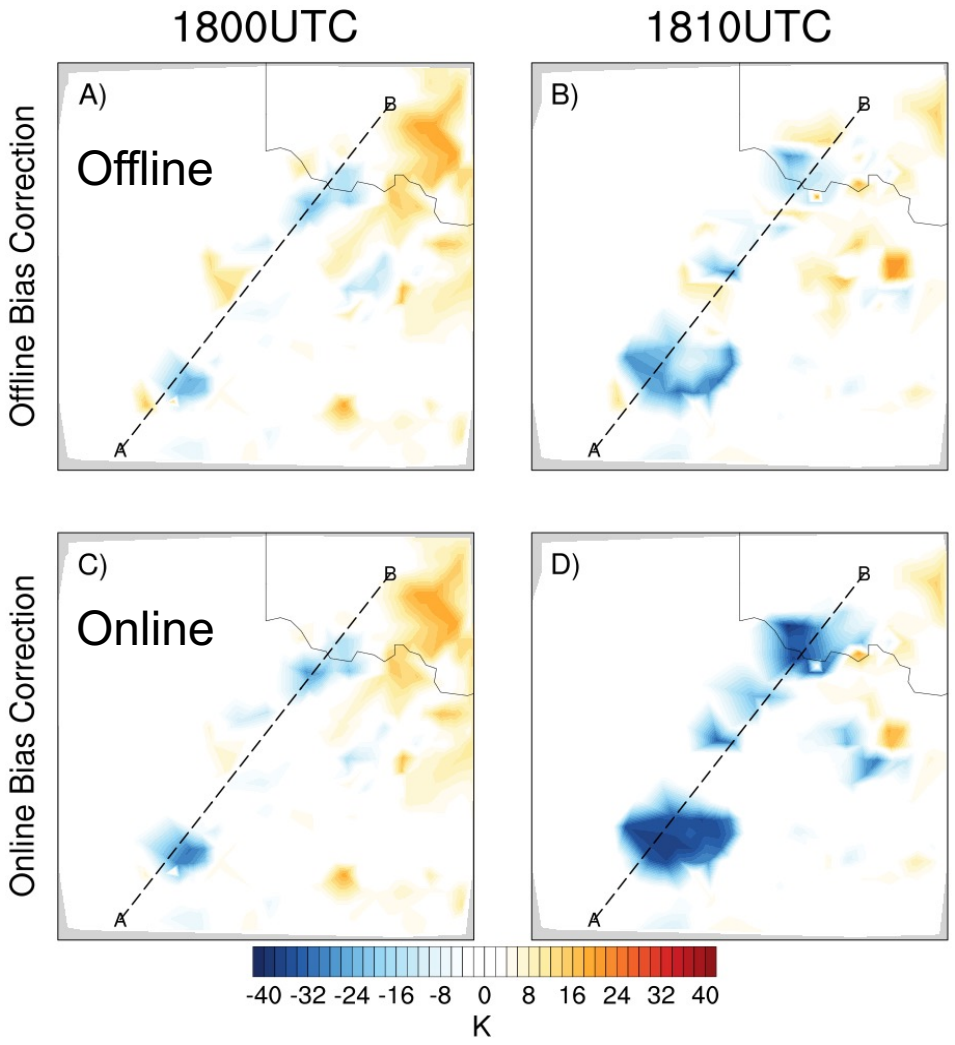

- The estimated bias in the offline approach includes a larger contribution from the model bias, which in this case is the underestimation of storm by the model
- The offline bias correction approach removes a large part of the innovation as bias as shown by a smaller bias corrected innovation.
- The online approach retains most of the negative innovation over the observed storm region
- Detailed diagnostics show that the online approach is able to more appropriately increment the moisture, hydrometeor and w fields during the data assimilation cycling, which lead to better subsequent forecasts.

Chandramouli et al. (2021; JAMES)

Outline

- Case study overview
- Part 1: Additive inflation, adaptive observation error, and different ABI channels (Johnson et al 2021)
- Part 2: offline vs. online nonlinear bias correction (Chandramouli et al. 2021)
- Summary and plans

Summary and plans

Summary

- **Impact of additive inflation, adaptive observation error, and different ABI channels**
  - Additive inflation and adaptive observation error approaches both show benefit to ABI all sky radiance DA to the subsequent storm
  - Channel 9 radiance DA improved forecast lead time by about 10 minutes compared to channel 10 radiance DA by strengthening upper level shortwave in clear air.
- **Impact of online bias correction**
  - Online non-linear bias correction for all-sky ABI radiance DA is developed in rapidly cycled EnKF system.
  - With RADAR reflectivity as anchor observation, the online bias correction improves background and analysis cloud regions.
  - The effect is accumulated during the DA cycling that is responsible for the superior forecast of the supercells

Ongoing work and future plans by OU MAP:

- Study ongoing to investigate interactions between ABI radiance DA and microphysics scheme errors, and to improve consistency between microphysics assumptions and observation operator assumptions, for an MCS case study.
- The online non-linear bias correction for all-sky radiances is also being implemented in EnVar
- Application of bias correction to multiple water vapor sensitive ABI channels
- Studies are underway to compare the vertical localization in EnKF and EnVar for convective scale ABI all-sky radiance DA
- Efforts are ongoing to develop the ABI all sky radiance DA in FV3-LAM, the US next generation convection allowing data assimilation and modelling system

Extra Slides

Results during DA cycling

- DA diagnostics stabilize by ~1800 UTC.
- Case was selected because of challenges of assimilating storms when all ensemble members fail to initiate the storms
- Under-dispersion remains a concern, but is common to all experiments

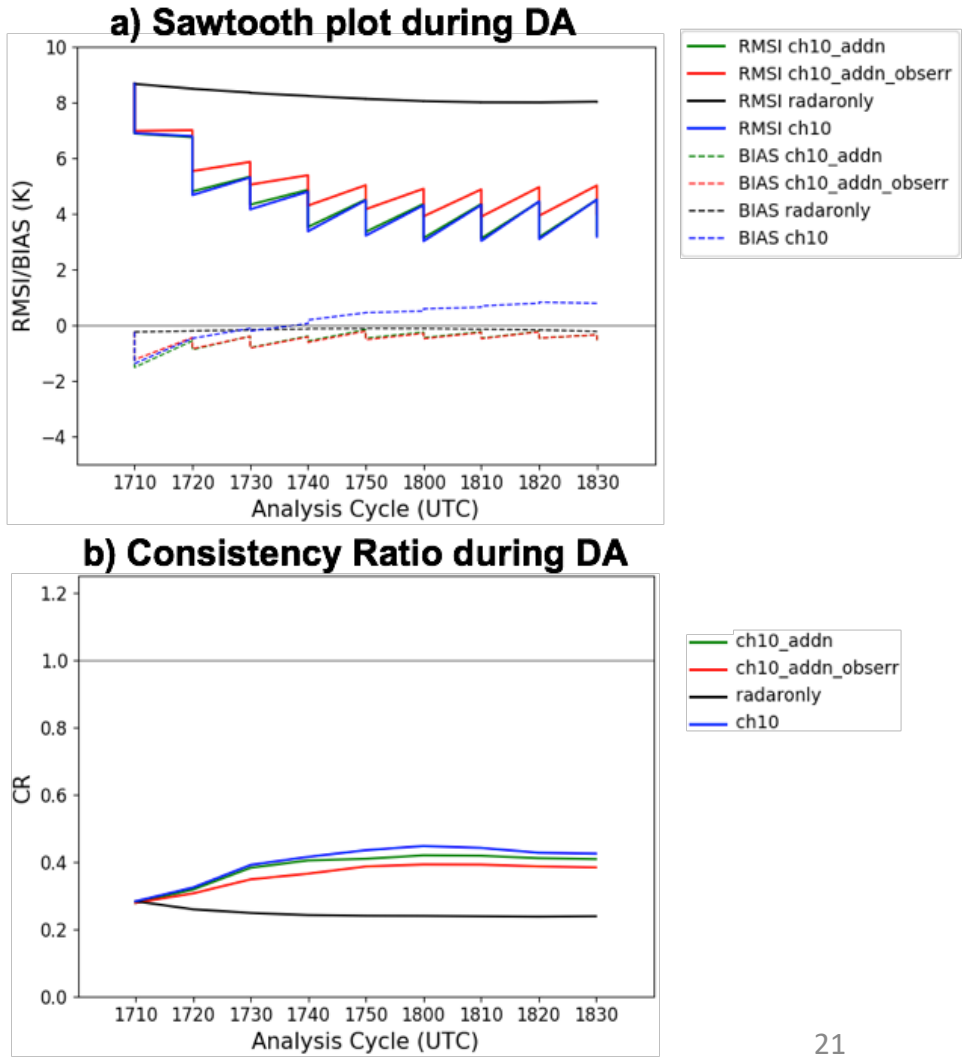

Johnson et al. (2021; JGR-atmos.)

Bias correction approaches

- **Non-linear offline bias correction:**

- Statistics of first-guess departures (O-B) are used to estimate the bias.
- Can not distinguish bias in the obs and bias in the model
- The non-linear offline approach by Otkin et al. (2018) represents fitting a polynomial function of bias predictors to the model first-guess departure.

Observation departure: d**Y** = y –h(x)

$$d\boldsymbol{Y} = [b_0 + b_1(z_i - c) + b_2(z_i - c)^2 + b_3(z_i - c)^3] \ , i = 1 \ to \ m$$

z -> bias predictor, b_0,b_1,b_2 and b_3 -> bias coefficients

In matrix form,

$$d\boldsymbol{Y} = \boldsymbol{Ab}$$

The solution to the above system is given by,

$$\boldsymbol{b} = [\propto \boldsymbol{I} + \boldsymbol{A}^T\boldsymbol{A}]^{-1}\boldsymbol{A}^T d\boldsymbol{Y}$$

Bias correction approaches

❑ **Non-linear online bias correction:**

➢ The bias is estimated at each analysis step along with the estimated state.

The coupled state and bias update step (Fertig et al. 2009) in EnKF :

Bias $b(p(\boldsymbol{x_b}), \beta) = p_1(\boldsymbol{x_b})\beta_1 + p_2(\boldsymbol{x_b})\beta_2 + p_3(\boldsymbol{x_b})\beta_3 + \ldots$

$\delta\boldsymbol{x} = \boldsymbol{K}(\boldsymbol{y} - \overline{\boldsymbol{Hx_b}} + b(p(\boldsymbol{x_b}), \delta\beta))$ where $\overline{\boldsymbol{Hx_b}} = \boldsymbol{Hx_b} - b(p(\boldsymbol{x_b}), \beta)$

$$\delta\beta = \left(\boldsymbol{P_\beta^b}^{-1} + \boldsymbol{pR^{-1}p^T}\right)^{-1} \boldsymbol{pR^{-1}}((\boldsymbol{y} - \overline{\boldsymbol{Hx_b}}) - \boldsymbol{H\delta x})$$

Starting with $\delta\boldsymbol{x}$=0 , $\delta\beta$=0 : The equations are solved iteratively.

➢ Past studies have revealed the co-existence of an unbiased anchor observation along with bias corrected observation can help distinguish the model and observation component of the biases, which in turn gives better analysis and forecast (Eyre 2016).

➢ The default bias correction in EnKF was modified to accommodate the non-linear cubic polynomial function for ABI radiances similar to the offline approach

Offline vs Online bias correction

first guess

Probability distribution of channel 9 ABI first-guess departures (B-O)

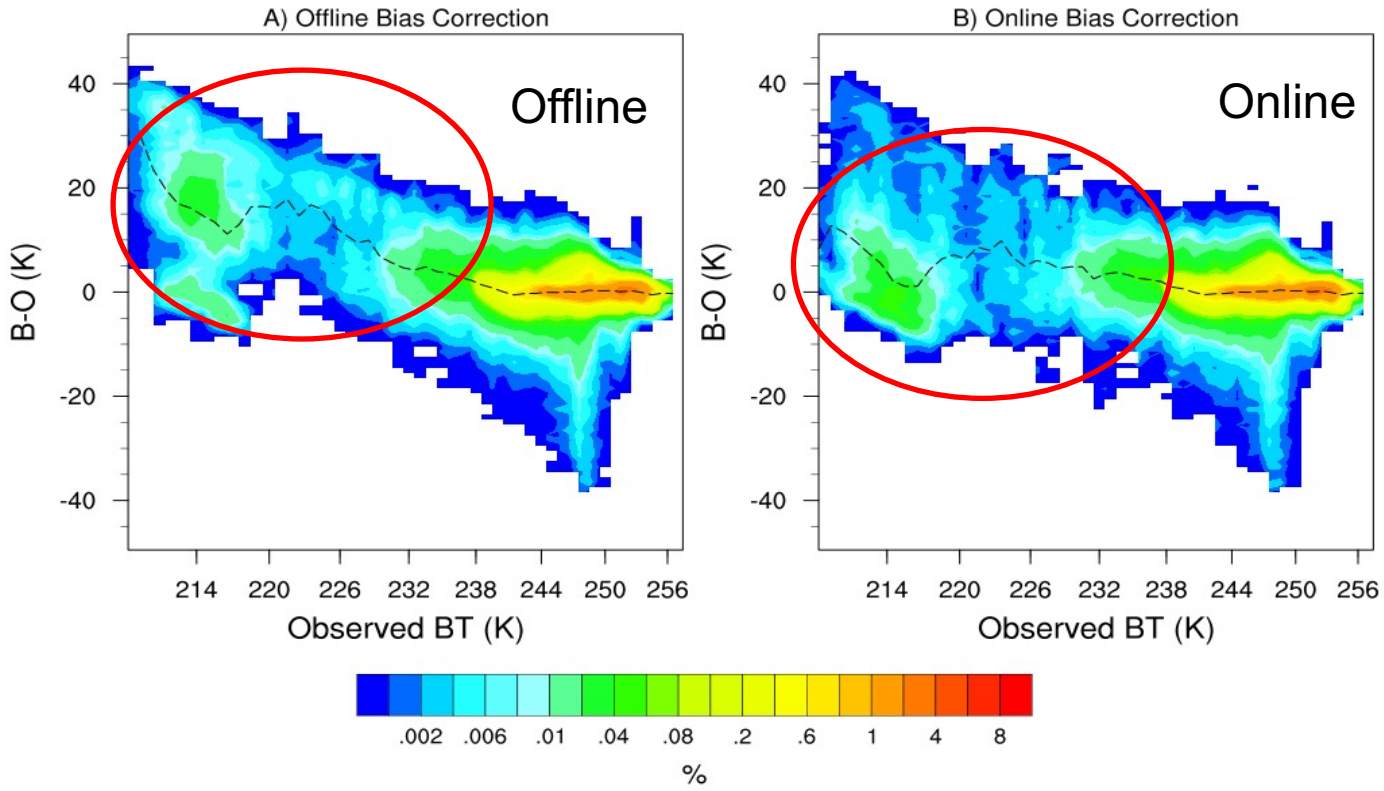

- The online approach exhibits less systematic deviation over the cloudy region (observed BT <=239K) than offline approach.
- This result suggests the effectiveness of using the radar reflectivity as anchoring observation to analyze the observed cloudy regions .

Chandramouli et al. (2021; JAMES)

More realistic storm structure from dBZ than ABI as storm matures

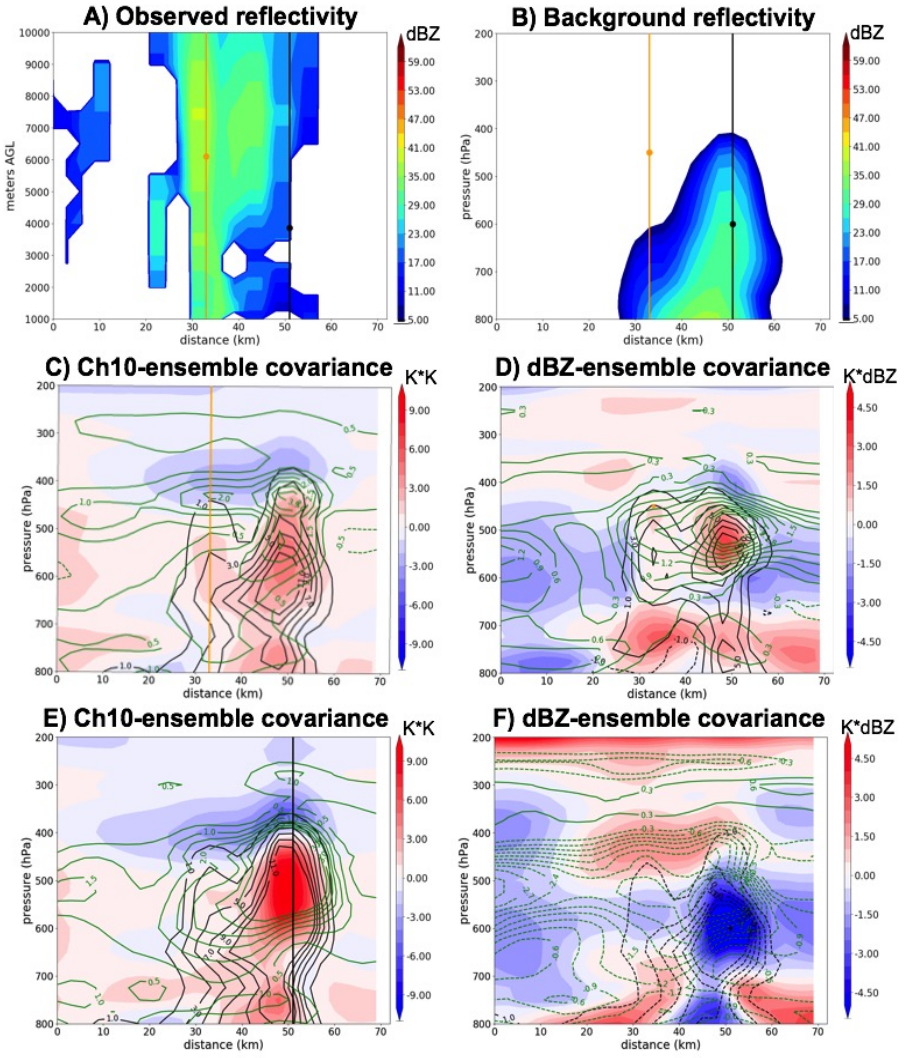

Panels (a) and (b) show cross-sections of reflectivity along the blue line in Figure 7d for (a) MRMS observations and (b) ensemble mean background in the 1810 UTC cycle of the *ch10_addn_obserr* experiment. Panels (c) and (d) are corresponding cross-sections of the background error covariance between temperature (shaded; K*K and dBZ*K, respectively), water vapor mixing ratio (green; K g kg^{-1} and dBZ g kg^{-1}, respectively, with zero lines suppressed) and total cloud condensate (black; K g kg^{-1} and dBZ g kg^{-}, respectively, with zero lines suppressed) and the ensemble priors of the (c) radiance observation at the location of the vertical orange line and (d) reflectivity observation at the location of the orange dot. Panels (e) and (f) are the same as in (c) and (d), except using the (e) radiance observation at the vertical black line and (f) reflectivity observation at the black dot.

ABI Ch. 9 provide information about clear air structure of shortwave

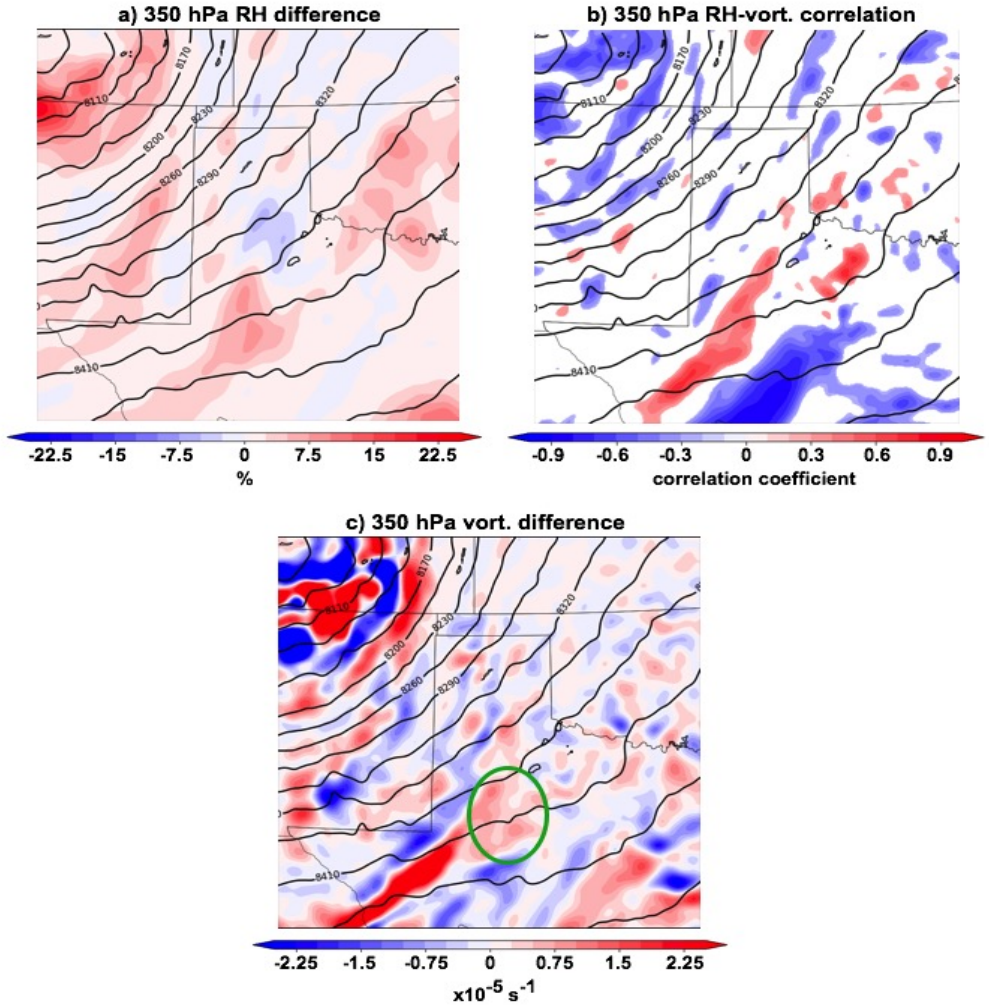

(a) 1800 UTC ensemble mean background difference of *ch9_addn_obserr* minus ch10_addn_obserr relative humidity (%) at 350 hPa. (b) ch10_addn_obserr background ensemble correlation between relative humidity and absolute vorticity perturbations. (c) as in (a) except for absolute vorticity ($x10^{-5}$ s^{-1}). All difference values are smoothed with Gaussian smoother with spatial scale of 15 km and MRMS composite reflectivity (black contours every 20 dBZ) at 1800 UTC is overlaid on all panels. Correlation in panel (b) is only plotted where the magnitude is statistically significant at the 90% confidence level.